Seed predation-induced Allee effects, seed dispersal and masting jointly drive the diversity of seed sources during population expansion

Violette Doublet, Lionel Roques, Etienne K Klein, François Lefèvre, Thomas Boivin

▶ **To cite this version:**

Violette Doublet, Lionel Roques, Etienne K Klein, François Lefèvre, Thomas Boivin. Seed predation-induced Allee effects, seed dispersal and masting jointly drive the diversity of seed sources during population expansion. 2023. hal-03768265v2

HAL Id: hal-03768265
https://hal.inrae.fr/hal-03768265v2

Preprint submitted on 25 Aug 2023

HAL is a multi-disciplinary open access archive for the deposit and dissemination of scientific research documents, whether they are published or not. The documents may come from teaching and research institutions in France or abroad, or from public or private research centers.

L'archive ouverte pluridisciplinaire **HAL**, est destinée au dépôt et à la diffusion de documents scientifiques de niveau recherche, publiés ou non, émanant des établissements d'enseignement et de recherche français ou étrangers, des laboratoires publics ou privés.

Distributed under a Creative Commons Attribution - NonCommercial 4.0 International License

Preprint

Seed predation-induced Allee effects, seed dispersal and masting jointly drive the diversity of seed sources during population expansion

Violette Doublet* · **Lionel Roques*** · **Etienne K. Klein** · **François Lefèvre** · **Thomas Boivin**

Abstract The environmental factors affecting plant reproduction and effective dispersal, in particular biotic interactions, have a strong influence on plant expansion dynamics, but their demographic and genetic consequences remain an understudied body of theory. Here, we use a mathematical model in a one-dimensional space and on a single reproductive period to describe the joint effects of predispersal seed insect predators foraging strategy and plant reproduction strategy (masting) on the spatio-temporal dynamics of seed sources diversity in the colonisation front of expanding plant populations. We show that certain foraging strategies can result in a higher seed predation rate at the colonisation front compared to the core of the population, leading to an Allee effect. This effect promotes the contribution of seed sources from the core to the colonisation front, with long-distance dispersal further increasing this contribution. As a consequence, our study reveals a novel impact of the predispersal seed predation-induced Allee effect, which mitigates the erosion of diversity in expanding populations. We use rearrangement inequalities to show that masting has a buffering role: it mitigates this seed predation-induced Allee effect. This study shows that predispersal seed predation, plant reproductive strategies and seed dispersal patterns can be intermingled drivers of the diversity of seed sources in expanding plant populations, and opens new perspectives concerning the analysis of more complex models such as integro-difference or reaction-diffusion equations.

Keywords Species interactions · Demogenetics · Foraging strategy · Founder effect · Rearrangement inequalities

Mathematics Subject Classification (2010) 92-10 · 92D25 · 26D15

F. Lefèvre and T. Boivin
INRAE, UR 629 Recherches Forestières Méditerranéennes, 84914 Avignon, France
E-mail: thomas.boivin@inrae.fr, and francois.lefevre.2@inrae.fr

L. Roques and E. K. Klein
INRAE, BioSP, 84914, Avignon, France
E-mail: lionel.roques@inrae.fr and etienne.klein@inrae.fr

V. Doublet,
Department of Ecology and Genetics, Evolutionary Biology Centre, Uppsala University, Uppsala, Sweden
E-mail: doublet.violette@gmail.com
* These authors contributed equally to the work.

Funding

The project leading to this publication has received funding from the ANR project RESISTE (ANR-18-CE45-0019). The study was also funded by the EU ERA-NET BiodivERsA Project SPONFOREST (BiodivERsA3-2015-58).

Conflict of interest

The authors declare that they have no conflict of interest.

Availability of data and material

Not applicable.

Code availability

All of the Matlab source codes used to generate the analyses conducted here are available at `https://doi.org/10.17605/OSF.IO/KWP4A`.

1 Introduction

Expansion of natural populations in concert with genetic differentiation is a crucial demographic process shaping the evolutionary potential, resilience and persistence of plant species. However, contemporary changes in the biotic and abiotic environment related to biological invasions, emerging diseases, climate and land-use changes are increasingly impacting the ability of species to colonise and persist in novel territories [8]. Assessing the demographic and genetic impacts of species' interactions during population expansion is one major issue for the forecasting of population spatio-temporal dynamics and their potential long-term consequences on ecosystems [11]. Those interactions impacting specifically population genetic diversity structures, and therefore future evolutionary potential, have been poorly investigated so far [21,30,38,39,62]. In keystone and long-lived plants such as trees, the ecological processes interfering with expansion are also related to population adaptive capacity in the context of contemporary changes [33,34,48]. Identifying the processes that shape spatial genetic structure in expanding plant populations is therefore of high importance. Aside from inherent demographic properties of the plant population, external features such as biotic interactions can have a significant effect on the process of expansion and the resulting diversity pattern. The interactions between plants and insects that feed on them are well acknowledged drivers of plant population dynamics [29,40], but their demographic and genetic consequences remain an understudied body of theory.

Range expansions are often associated with a loss of genetic diversity towards expansion fronts due to successive founder effects that may result from a greater contribution of individuals located at the leading edge of the population to the expansion area [47,49,58]. In other words, the diversity of seed sources that effectively contribute to the expansion front is a primary driver of the genetic diversity in the future expanded population. Such successive founder effects can lead to a surfing phenomenon when a mutation arising in the front progressively invades the expansion area [14]. Alternatively, founder effects may be mitigated by propagule dispersal patterns and/or by decreased fitness of front individuals due to environmental factors. First, local conditions in

the front may reduce a species' dispersal ability [1]. Second, a species' propensity to disperse propagules at long-distance increases the contribution of the high density of individuals in the core to the expansion front, thus reducing the founder effect at the front [2,7,15,24,41,42]. Third, population growth rate at the front can be lower than in the core due to unfavourable environmental conditions [18,50], to stronger interactions with other species (e.g. interspecific competition, [54]), or to Allee effects, i.e. a decrease in individual fitness at low population density [9,53]. Predator-prey relationships can be key sources of Allee effects in animal populations [6, 19,32], but similar evidence is yet very limited in annual plants [63] and to our knowledge non-existent in perennial plants.

Here, we investigate the mechanisms through which the diversity of seed sources in the expansion front is driven by interference between the foraging strategy of a seed predator insect and the reproduction strategy of the plant. Interestingly, seed predation by insects is close to predator-prey relationships because insects immediately kill individuals (i.e. embryos) in the plant population [3]. We also consider plant demographic features associated with seed production and seed dispersal as they are major determinants of seedling recruitment and subsequent spatial structure and distribution [43]. A first feature refers to the masting and non-masting strategies, which reflect inter-annual patterns of seed production in perennial plants that can be highly variable [10,25,26,57] or stable [55,60], respectively. A second feature refers to long-distance dispersal, which affects spatial genetic structures through more diversified origins of dispersed seeds far away from the population core [27] and alters the speed at which expansion occurs [16,31,35].

Recent modelling approaches have used population-scale continuous-time continuous-space models, such as reaction-diffusion and integro-differential equations, to study the joint effects of dispersal and growth processes on the dynamics of neutral diversity during an expansion process, over several generations (e.g. [5,18,21,53]). Here, we develop a simple but analytically tractable discrete-time continuous-space model over a single reproductive period to assess the consequences of predispersal seed predation rate, spatial distribution of predators, seed dispersal and masting on the diversity of seed contributors to the expansion zone. We first analyse the occurrence of an Allee effect in the plant population depending on the functional relationship (sublinear or superlinear relationships, corresponding to different foraging strategies) between the predator density and the plant density. We use Hardy-Littlewood type rearrangement inequalities to assess the effect of masting on the strength of the Allee effect. Next, we describe seed dispersal with a convolution kernel to assess the respective contributions of individuals to the expansion, depending on their position in the population and on the type of dispersal kernel (thin-tailed or fat-tailed). We assess plant population diversity in the expansion zone through the diversity of seed sources that contribute to the expansion.

2 Material and methods

The objective of the model is to assess the origin of seeds received at each spatial position in one year, or averaged over several years in case of fluctuating seed production, under different patterns of seed production, seed dispersal kernel and spatial distribution of seed predation rates. To achieve this goal, we use an analytical approach, in a one-dimensional space.

2.1 Seed production

The plant density is represented by a function $a(x) > 0$, $x \in \mathbb{R}$ being the position. As we focus on an expanding population, we assume that the plant density decays away from the center

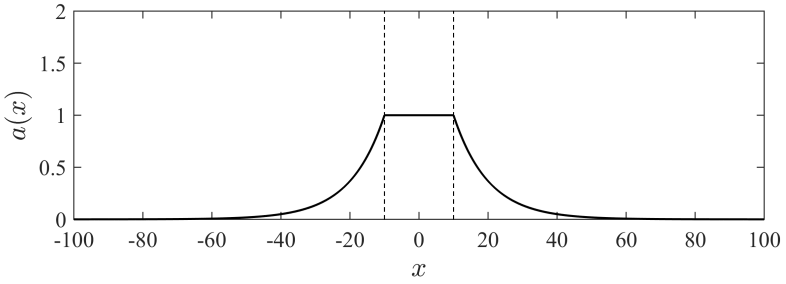

Fig. 1 Example of plant density $a(x)$. The region between the dotted lines corresponds to the "core" of the plant population, $(-L, L)$. In this particular example, $L = 10$ and the plant density decays exponentially outside of this region ($a(x) = \exp(-(|x| - L)/10)$ for $|x| > L$).

point 0, which represents the middle of the core of the population. A schematic example that we used in our numerical computations is given in Fig. 1. In this example, the plant density is constant in the "core" $(-L, L)$, meaning that plant density has reached the carrying capacity of the environment, and then decays exponentially.

We always assume that the individual seed production per plant is spatially homogeneous. Regarding the temporal variations in seed production, we consider two scenarios.

Assumption 1 (Non-masting scenario)**.** The individual seed production is constant, $r_k = r \geq 0$ seeds per plant per year, independently of the year k.

Assumption 2 (Masting scenario)**.** The individual seed production varies periodically with a period of T years ($T \in \mathbb{N}^*$), i.e. $r_{k+T} = r_k$ for any year $k \in \mathbb{N}$. The mean individual seed production over one period of time T is denoted by:

$$\overline{r} := \frac{1}{T} \sum_{k=1}^{T} r_k. \tag{1}$$

For simplicity, we assume that $r_k > 0$ in all of the formulas presented below. Actually, the occurrence of years with a null seed production does not modify our results. Note that, in the masting scenario, the plant population density $a(x)$ remains unchanged over the time period $k = 1, \ldots, T$. This means that the seeds do not contribute to the plant population during this period, due to a non-reproductive juvenile stage of at least T years (otherwise, competition between juveniles and between juveniles and adults should be considered, leading to a more complex and less analytically tractable model). Also, even if there is probably a trade-off between growth and reproduction that would induce variation in the average number of seeds over the lifetime of the plant, we do not consider it in our modelling approach.

2.2 Seed predation scenarios

The correlation between seed predator density $p(x)$ and plant density $a(x)$ depends on biological features that involve the foraging strategy of seed predators. A first foraging strategy includes seed predators that display a high mobility allowing a rapid diffusion in the landscape without any influence of plant density. This leads to a spatially homogeneous distribution of the seed predators within their host population. A second foraging strategy is characterised by a positive

correlation between seed predator density and plant density, which can result from reduced seed predator dispersal under higher density of plants (e.g., due to attraction or impaired mobility).

As a reference, we use a null scenario, i.e. without seed predators (no seed predation, $p \equiv 0$). According to the seed predator foraging strategies, we then define two seed predation scenarios (*Sublinear* and *Superlinear*) which describe the dependence of the density of predators $p(x)$ with respect to the plant density $a(x)$, through some positive and differentiable function μ. Namely,

$$p(x) = \mu(a(x))\, r \text{ (without masting) or } p_k(x) = \mu(a(x)) r_{k-d} \text{ (with masting).} \tag{2}$$

With masting, the seed production is variable, and the number of seed predators of year k is proportional to the number of seeds of year $k-d$, where $d \in \mathbb{N}$ is the duration of an obligatory period of larval developmental arrest, namely larval diapause [3], $d = 2$ years in our computations. We assume that $\mu \in C^1(0,\infty)$, $\mu \geq 0$ and either Assumption 3 or 4.

Assumption 3 (Sublinear seed predation)**.** In this case, $a \mapsto \mu(a)/a$ is strictly decreasing on $[0, +\infty)$.

This means that seed predator density does not increase too fast with the plant density. In this scenario, either the seed predator density tends to decrease as the plant density increases, or it slowly increases (i.e., sublinearly) with the plant density. This assumption encompasses the case of decreasing functions $\mu(a)$ or slowly increasing functions, e.g., $\mu(a) = \sqrt{a}$. An important subcase corresponds to the *homogeneous seed predation scenario*, where μ is constant, and p is spatially constant and proportional to the number of produced seeds $p(x) = \mu\, r$ ($\mu = 1$ in our computations).

Assumption 4 (Superlinear seed predation)**.** In this case, $\mu(0) = 0$ and $a \mapsto \mu(a)/a$ is nondecreasing (i.e., increasing but not necessarily strictly) on $[0, +\infty)$.

Here, the seed predator density increases superlinearly as the plant density increases. This assumption includes the assumption of a *proportional seed predation*, where $\mu(a) = \mu\, a$ is proportional to a and $\mu(a)/a = \mu$ is constant. In this case, the density of seed predators increases linearly with the plant density: $p(x) = \mu\, a(x)\, r$ (or $p_k(x) = \mu\, a(x)\, r_{k-d}$, with masting).

2.3 Seed predation rate

We assume that the proportion of predated seeds f only depends on the ratio $\rho = p/(r\, a)$ between the density of seed predators and the number of available seeds. We then assume a general increasing function f for the proportion of predated seeds ($f' > 0$, $f(0) = 0$, $f(\infty) \leq 1$). The density of viable seeds $s(x)$ produced at a position x in the absence of masting is equal to the density of seeds ($r\, a(x)$) multiplied by the fraction of viable seeds ($1 - f$):

$$s(x) = r\, a(x) \left(1 - f\left(\frac{p(x)}{r\, a(x)}\right)\right) = r\, a(x) \left(1 - f\left(\frac{\mu(a(x))}{a(x)}\right)\right). \tag{3}$$

In the presence of masting, we compute the average density of viable seeds over one period, i.e., we use the same formula as above, averaged over T years:

$$\overline{s}(x) = \frac{1}{T} \sum_{k=1}^{T} r_k\, a(x) \left(1 - f\left(\frac{p_k(x)}{r_k\, a(x)}\right)\right) = \frac{1}{T} \sum_{k=1}^{T} r_k\, a(x) \left(1 - f\left(\frac{r_{k-d}\, \mu(a(x))}{r_k\, a(x)}\right)\right). \tag{4}$$

For some results, we need a more explicit form for the function f, such that when the ratio ρ is very large, the proportion of predated seeds approaches 1, and when ρ is low, it is proportional to ρ. We considered here one of the simplest relationships satisfying these properties:

$$f(\rho) = \frac{\rho}{(\theta^{-1} + \rho)}, \tag{5}$$

with a constant $\theta > 0$ ($\theta = 2$ in our computations; $f(\rho) \sim \theta\rho$ for small ρ). With this form for the function f, we have:

$$s(x) = r\,a(x)\left(1 - f\left(\frac{p(x)}{r\,a(x)}\right)\right) = \frac{(r\,a(x))^2}{r\,a(x) + \theta p(x)}, \tag{6}$$

and in the presence of masting:

$$\overline{s}(x) = \frac{1}{T}\sum_{k=1}^{T} r_k\,a(x)\left(1 - f\left(\frac{p_k(x)}{r_k\,a(x)}\right)\right) = \frac{1}{T}\sum_{k=1}^{T}\frac{(r_k\,a(x))^2}{r_k\,a(x) + \theta p_k(x)}. \tag{7}$$

2.4 Seed dispersal

The model focuses on the dispersal of seeds that escaped predispersal insect seed predation, which are referred to as viable seeds. Viable seeds are dispersed according to a symmetrical kernel $J(x)$. By 'kernel', we mean here that J is a positive, measurable, even function of mass 1, which decays away from 0. The density of seeds received at a position x from a source position in y is proportional to $J(x-y)$. We compare the relative contribution of different seed sources in the plant population as follows: considering two source positions x_A and x_B, given the density of viable seeds $s(x_A)$ and $s(x_B)$ produced at x_A and x_B, the ratio of viable seeds received at x, from one source position to the other is:

$$\frac{J(x - x_A)\,s(x_A)}{J(x - x_B)\,s(x_B)}. \tag{8}$$

The first factor $J(x-x_A)/J(x-x_B)$ and its dependence with respect to the dispersal kernel have already been well-studied in [27]. Thin-tailed and fat-tailed kernels can be defined by the way they decay to 0 as $x \to \pm\infty$. Thin-tailed kernels decay faster than any exponential function, i.e., for all $\eta > 0$, $J(x)\,e^{\eta\,|x|} \to 0$ as $x \to \pm\infty$. On the opposite, fat-tailed kernels decay slower than any exponential function does (e.g., [16,27,31]): for all $\eta > 0$, $J(x)\,e^{\eta\,|x|} \to +\infty$ as $x \to \pm\infty$.

In particular, for a spatially-homogeneous individual seed production ($s(x_A) = s(x_B)$), fat-tailed kernels that produce more long-distance dispersal also lead to more mixing than thin-tailed kernels. More precisely, if $x_A < x_B$, [27] showed that for a large class of thin-tailed kernels, only the more proximal source (x_B) contributes to the positions $x \gg x_B$ far away from both sources (only x_A contributes for $x \ll x_A$):

$$J(x - x_A)/J(x - x_B) \underset{x\to+\infty}{\longrightarrow} 0 \text{ and } J(x - x_A)/J(x - x_B) \underset{x\to-\infty}{\longrightarrow} +\infty.$$

Conversely, both sources contribute to any position with all of the fat-tailed kernels considered in [27], even far away from the sources, which means that $J(x-x_A)/J(x-x_B)$ converge to positive constants as $x \to \pm\infty$. Their respective contributions depend on the precise shape of the kernel.

For instance, the exponential power kernel ($\alpha, \beta > 0$)

$$J(x) = \frac{\beta}{2\,\alpha\Gamma(1/\beta)}\,e^{-\left(\frac{|x|}{\alpha}\right)^{\beta}}$$

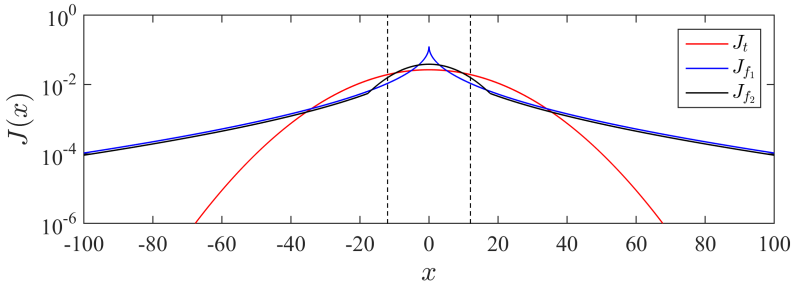

Fig. 2 Dispersal kernels. J_t is a thin-tailed Gaussian kernel, J_{f_1} a fat-tailed exponential power kernel with power 1/2 and J_{f_2} a fat-tailed which behaves as J_{f_1} for large x but is not peaked at 0. The vertical dotted lines correspond to the mean dispersal distance, $\overline{d}(J) = 12$m, common to the three kernels. The parameter values are given in the text.

is able to move between the two regimes, depending on the power β: when $\beta > 1$, J is a thin-tailed kernel, while it is a fat-tailed kernel when $\beta < 1$ [27]. The exact exponential case ($\beta = 1$) is more ambiguous, as it shares some properties of both types of kernels: it leads to a mixing of propagules [27], but also to a constant speed of expansion [16] (see Appendix 1 for some results in the particular case $\beta = 1$). Here, we use a standard Gaussian kernel ($\beta = 2$) to illustrate the thin-tailed case:

$$J_t(x) = \frac{1}{\sigma\sqrt{2\pi}} e^{-\frac{x^2}{2\,\sigma^2}},$$

with $\sigma = \alpha/\sqrt{2}$. For the fat-tailed case, we use a power $\beta = 1/2$:

$$J_{f_1}(x) = \frac{1}{4\,\alpha} e^{-\sqrt{\frac{|x|}{\alpha}}}.$$

Due to its form at 0, this standard fat-tailed kernel tends to disperse a very large amount of seeds around the origin. To avoid this effect, we also consider another fat-tailed kernel, which has the same tail as J_{f_1}, but is smooth and not "peaked" around 0:

$$J_{f_2}(x) = \begin{cases} \frac{1}{\gamma\, C\sqrt{2\pi}}\, e^{-\frac{x^2}{2\,\gamma^2}} & \text{for } |x| < x_0 \\ \frac{1}{4\,C\,\alpha} e^{-\sqrt{\frac{|x|}{\alpha}}} & \text{for } |x| \geq x_0 \end{cases}$$

with $x_0 > 0$ such that J_{f_2} is continuous and decreasing away from 0 and $C > 0$ a constant such that the kernel J_{f_2} is of integral 1. This kernel is simply a combination of the thin-tailed kernel J_t around the origin, and of the fat-tailed kernel J_{f_1} far from the origin. As our objective here is to understand the effect of long-distance dispersal (i.e. the dispersal tail) independently of the mean dispersal distance, we fixed the parameters of the kernels such that they share the same mean dispersal distance:

$$\overline{d}(J) := \int_{\mathbb{R}} |x|\, J(x)\, dx.$$

In particular, we have $\overline{d}(J_t) = \sigma\sqrt{2/\pi}$ and $\overline{d}(J_{f_1}) = 6\,\alpha$. In our computations, we used a mean dispersal distance of 12 (e.g., meters, although the exact unit is not important for our study). This leads to a value $\sigma = 15$ for J_t, and $\alpha = 2$ for J_{f_1}. For J_{f_2}, we used $\alpha = 2$, $\gamma = 9$ to get $\overline{d}(J_{f_2}) = 12$m. With these parameter values, we obtain $x_0 \approx 18$m. We depict in Fig. 2 the three kernels J_t, J_{f_1} and J_{f_2} associated with the above parameter values.

2.5 Distribution of the seed source locations

The distribution of the positions y of the sources of the viable seeds arrived at x is given by:

$$m_x(y) := \frac{s(y)\, J(|x-y|)}{\int_{\mathbb{R}} J(|x-v|)\ s(v)\, dv}, \tag{9}$$

with $s(v)$ the viable seeds produced at the position v (summed over one period in the presence of masting). This distribution informs us about the position of the main contributors to population expansion at each position x. In particular, it tells whether the contributors are close to the position x or not, and if they are concentrated around some particular location, or more widely distributed.

2.6 Summary of the model

- The plant density is represented by a function $a(x) > 0$ which decays away from the center point 0. The individual plant seed production does not depend on the space, x and is either a constant r (non-masting scenario, Assumption 1) or varies periodically with a period of T years, i.e. $r_{k+T} = r_k$ (masting scenario, Assumption 1).
- The density of predators is represented by a function $p(x)$. In the absence of predators, $p \equiv 0$. Otherwise, $p(x)$ depends on the local plant density, through a function $\mu(a)$. This function $\mu(a)$ defines the seed predation scenario (Assumptions 3 and 4). With masting, the density $p_k(x)$ of seed predators of year k depends on the number of seeds of year $k-d$, where d is the diapause duration, see (2).
- At each position, before dispersal, a proportion $f(p(x)/(ra(x)))$ of the seeds are predated (or $f(p_k(x)/(r_k a(x)))$ in the presence of masting), with f a positive increasing and differentiable function which we may assume to be generic ($f' > 0$, $f(0) = 0$, $f(\infty) = 1$) for some results or defined by (5) for other results.
- The density of viable seeds $s(x)$ in the absence of masting is equal to the density of seeds $(r\, a(x))$ multiplied by the fraction of viable seeds $(1-f)$, see eq. (3). In the presence of masting, we consider the average density of viable seeds over one period, $\overline{s}(x)$, see eq. (4).
- These seeds are dispersed according to a dispersal kernel J, which may be thin-tailed or fat-tailed.

3 Results

3.1 Allee effect induced by seed predation

We begin by analysing whether seed predation induces an Allee effect under our model assumptions. At this stage, we do not need to take dispersal into account, as we only focus on seed production. Thus, we simply consider the number of viable seeds per plant, i.e., the ratio $s(x)/a(x)$ and we study how this ratio depends on the plant density $a(x)$. By definition, an Allee effect occurs if there is a positive dependence between these two quantities, i.e., if s/a is a strictly increasing function of a.

No seed predation. In the absence of seed predators, the number of viable seeds per plant is simply the number of seeds $s(x)/a(x) = r$ (or $\overline{r}$ the average individual seed production, in case of masting). Thus, viable seed production is independent of population density and no Allee effect occurs in this case.

Sublinear seed predation, without masting. Dividing (3) by a and differentiating with respect to a, we get:

$$\frac{\partial}{\partial a}(s/a) = -r\frac{\partial}{\partial a}\left(\frac{\mu(a)}{a}\right) f'\left(\frac{\mu(a)}{a}\right). \tag{10}$$

Under this scenario, $\mu(a)/a$ is a strictly decreasing function, thus $\partial/\partial a(\mu(a)/(a)) < 0$. Since $f' > 0$, the above quantity is positive. This means that s/a increases with the plant density a: this scenario induces an Allee effect. In the particular case with a homogeneous seed predation scenario ($p = \mu\, r$) and with the predation rate (5), we simply get (see Fig. 3):

$$\frac{s(x)}{a(x)} = r\,\frac{a(x)}{a(x) + \theta\,\mu}. \tag{11}$$

Sublinear seed predation, with masting. Dividing (4) by a and differentiating with respect to a, we get:

$$\frac{\partial}{\partial a}(\overline{s}/a) = -\frac{1}{T}\sum_{k=1}^{T} r_{k-d}\frac{\partial}{\partial a}\left(\frac{\mu(a)}{a}\right) f'\left(\frac{r_{k-d}\,\mu(a)}{r_k\, a}\right). \tag{12}$$

As $\mu(a)/a$ is a strictly decreasing function in this scenario, eq. (12) shows that $\overline{s}/a$ is an increasing function of a. Thus, there is an Allee effect. To analyse the effect of masting on the strength of the Allee effect, we need another assumption on f (which is satisfied in the particular case of eq. (5)). The function f is such that the proportion of predated seeds converges to 1 as the ratio between the density of seed predators and the number of available seeds becomes large, in the following way: $f(\rho) \sim 1 - C/\rho$, for some constant $C > 0$. At the limit of small plant density ($a \sim 0$), we therefore obtain:

$$\frac{\overline{s}(x)}{a(x)} \sim \frac{C\,a(x)}{\mu(0)}\frac{1}{T}\sum_{k=1}^{T}\frac{r_k^2}{r_{k-d}} \text{ as } a \to 0.$$

Then, we use the following rearrangement inequality (Hardy-Littlewood, see Section 4).

Lemma 1 *We have*

$$\overline{r} \leq \frac{1}{T}\sum_{k=1}^{T}\frac{r_k^2}{r_{k-d}}.$$

Thus, in the presence of masting, the slope of $\overline{s}/a$ (seen as a function of a) around $a = 0$ is increased compared to a situation without masting, where r_k is constant equal to $\overline{r}$ and therefore $s(x)/a(x) \sim C\ a(x)\overline{r}/\mu(0)$. This means that masting leads to a weaker Allee effect.

In the particular case with a homogeneous seed predation scenario ($p = \mu\, r$) and with the function f given by (5), we get

$$\frac{\overline{s}(x)}{a(x)} = \frac{1}{T}\sum_{k=1}^{T}\frac{r_k^2\, a(x)}{r_k\, a(x) + \theta\,\mu\, r_{k-d}}. \tag{13}$$

We then prove another rearrangement inequality (Section 4) which leads to the following lemma.

Lemma 2 *We have*

$$\frac{1}{T}\sum_{k=1}^{T}\frac{r_k^2\, a(x)}{r_k\, a(x) + \theta\,\mu\, r_{k-d}} \geq \overline{r}\,\frac{a(x)}{a(x) + \theta\,\mu}.$$

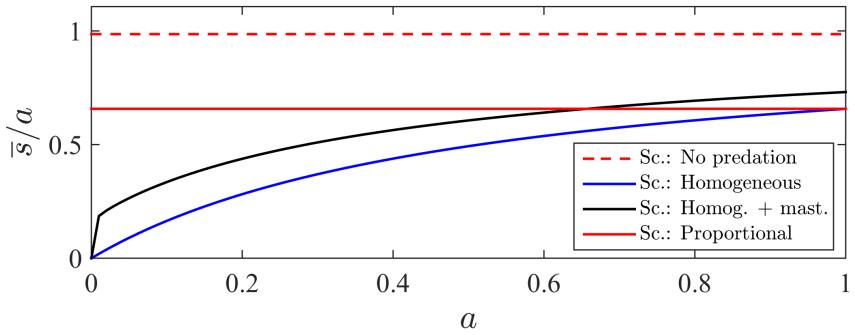

Fig. 3 Occurrence of an Allee effect: number of viable seeds per plant, in terms of the plant density a. We assume here of function f (proportion of predated seeds) of the form (5). We consider the following scenarios: without predation ($s/a = r$ or $\overline{s}/a = \overline{r}$ with masting); with homogeneous seed predation (s/a is given by (11)); with homogeneous seed predation and masting ($\overline{s}/a$ is given by (13)); with proportional seed predation ($s/a = r/(1+\theta\,\mu)$ and $\overline{s}/a = \overline{r}/(1+\theta\,\mu)$, with masting). The average seed production over one period of time is the same in the four scenarios. In the presence of masting, the individual seed production is given by $r_k = c\,(|\sin(\pi\,k/T)| + \varepsilon)$ (mean value $\overline{r} = c(0.64+\varepsilon)$). In the absence of masting, $r = \overline{r}$. The parameter values are $T = 7$, $\theta = 1/2$, $\mu = 1$ and $\varepsilon = 0.01$. Note that the four curves are proportional to c, which can therefore be arbitrarily fixed (here, $c = 1/0.64$).

In other words, the mean number of viable seeds per plant is always larger in the presence of masting, compared to the non-masting scenario with a constant individual seed production equal to $\overline{r}$ (see eq. (11)). This corresponds to a weaker Allee effect compared to scenario of homogeneous seed predation without masting, see Fig. 3.

Superlinear seed predation. Here, $\mu(a)/a$ is increasing (or constant), thus $\partial/\partial a(\mu(a)/(a)) \geq 0$. Using the expressions (10) and (12) we observe that $s(x)/a(x)$ (without masting) and $\overline{s}(x)/a(x)$ (with masting) are both decreasing functions of the plant density a. Thus, there is no Allee effect in this case.

3.2 Mixing of seeds from two sources

We now analyse the intertwined effects of the biotic Allee effect and seed dispersal, depending on the type of dispersal kernel. For simplicity, we make the Assumption (5) on the predation rate, and we consider two particular seed predation scenarios: the homogeneous seed predation scenario (subcase of the Assumption 3) and the proportional seed predation scenario (subcase of the Assumption 4).

We consider two seed source positions $0 \leq x_A < x_B$, so that $a(x_A) > a(x_B)$, and we study their respective contributions to population expansion at any location x. We recall that the ratio between the viable seeds received at a position x from the two positions x_A, x_B is given by eq. (8). To analyse the effects of the predation scenarios and of the occurrence of masting, we first focus on the ratio between the viable seeds produced by the two sources: $s(x_A)/s(x_B)$. Note that we do not need to make any assumption on the shape of the dispersal kernel at this stage, since the ratio $s(x_A)/s(x_B)$ is independent of the kernel J.

No seed predation. First, in the absence of seed predators, $s(x)/a(x) = r$, thus we obtain $s(x_A)/s(x_B) = a(x_A)/a(x_B)$: the ratio of viable seeds produced by the two sources is equal to

the ratio of the plant densities at each source position. The same formula holds in the presence of masting.

Homogeneous seed predation without masting. From eq. (11), we get:

$$\frac{s(x_A)}{s(x_B)} = \frac{a(x_A)}{a(x_B)} \frac{1+\theta\,\mu/a(x_B)}{1+\theta\,\mu/a(x_A)} > \frac{a(x_A)}{a(x_B)}, \tag{14}$$

thus, the relative contribution of the position x_A, where the seed source density is larger, is higher than without predation.

Homogeneous seed predation with masting. Similarly, using eq. (13), we obtain the ratio $\overline{s}(x_A)/\overline{s}(x_B))$ between the number of viable seeds produced at x_A and x_B, during a period of time T.

Lemma 3 *We have:*

$$\frac{a(x_A)}{a(x_B)} \leq \frac{\overline{s}(x_A)}{\overline{s}(x_B)} = \frac{a(x_A)}{a(x_B)} \frac{\frac{1}{T}\sum_{k=1}^{T} \frac{r_k^2}{r_k+\theta\,\mu\,r_{k-d}/a(x_A)}}{\frac{1}{T}\sum_{k=1}^{T} \frac{r_k^2}{r_k+\theta\,\mu\,r_{k-d}/a(x_B)}} \leq \frac{a(x_A)}{a(x_B)} \frac{1+\theta\,\mu/a(x_B)}{1+\theta\,\mu/a(x_A)}. \tag{15}$$

The left inequality simply follows from $a(x_A) > a(x_B)$. The right inequality is a consequence of a rearrangement inequality proved in Section 4. Thus, the relative contribution of the position x_A is still higher than without predation but lower than in the same scenario without masting (compare with eq. (14)).

Proportional seed predation with or without masting. In this case, we have $s(x_A)/s(x_B) = \overline{s}(x_A)/\overline{s}(x_B) = a(x_A)/a(x_B)$, as with no predation.

To illustrate these results with the three types of dispersal kernels considered, in Fig. 4, we depict the proportion of seeds from source x_A at any position x in the absence of masting,

$$\pi_A := \frac{J(x-x_A)\,s(x_A)}{J(x-x_A)\,s(x_A) + J(x-x_B)\,s(x_B)},$$

or, in the presence of masting,

$$\pi_A := \frac{J(x-x_A)\,\overline{s}(x_A)}{J(x-x_A)\,\overline{s}(x_A) + J(x-x_B)\,\overline{s}(x_B)},$$

with $x_A = 0$ (center of the core of the population) and $x_B = 20$ (inside the decreasing part of the front, see Fig. 1). Note that the values r and $\overline{r}$ of the individual seed production have no effect on the ratio π_A.

We observe that, whatever the dispersal kernel, the proportion of viable seeds received from x_A at positions far away from the sources ($x \gg 1$) is higher in scenario of homogeneous seed predation than in scenarios of no seed predation or proportional seed predation. In the presence of masting, this proportion takes intermediate values. Such observations corroborate the previous results demonstrated analytically. The source x_B is closer to the positions $x \gg 1$, but in scenario of homogeneous seed predation such contribution is compensated by the Allee effect generated by a higher seed predation rate per plant. This leads to a higher contribution of the source x_A in the core of the population. We previously showed analytically that the Allee effect was weaker in the presence of masting. Here, it leads to a lower contribution of the source x_A. Such contribution of the source x_A is however higher than in scenarios of no seed predation or proportional seed

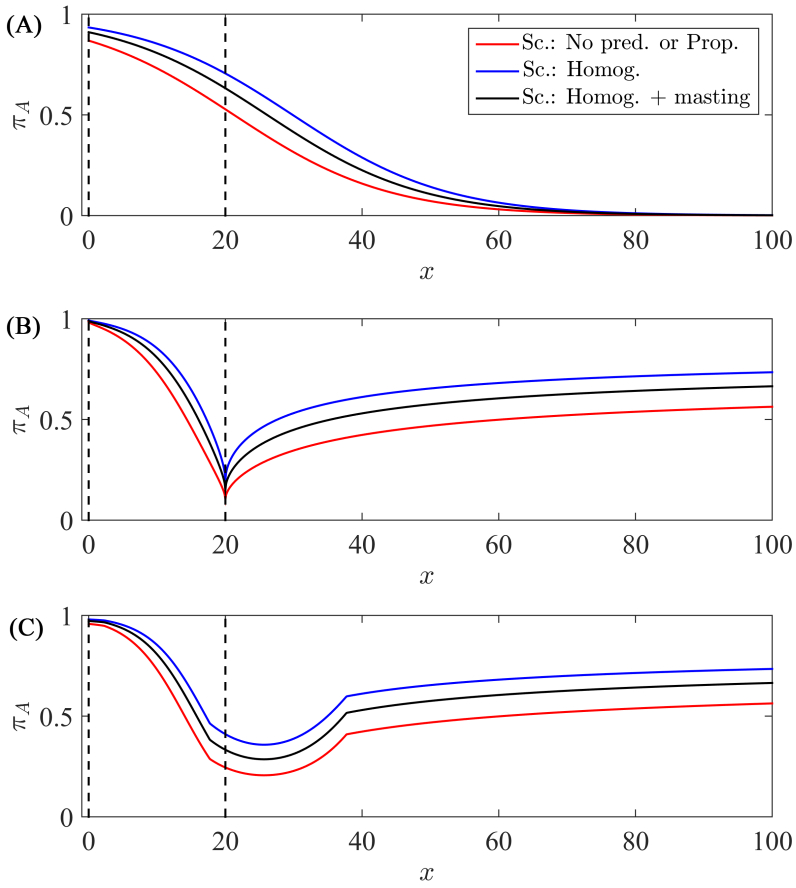

Fig. 4 Proportion π_A of seeds arriving in x from source x_A (at $x = 0$) compared to source x_B (at $x = 20$). The vertical dotted lines correspond to the positions x_A and x_B. Panel A corresponds to a thin-tailed kernel (J_t), Panel B to the fat-tailed kernel J_{f_1} and Panel C to the fat-tailed kernel J_{f_2}. The scenarios are: No seed predation, homogeneous seed predation with or without masting and proportional seed predation. In the presence of masting, the individual seed production r_k has the same sinusoidal shape as in Fig. 3.

predation. As already known [27], with a thin-tailed kernel (Panel A in Fig. 4), the proportion π_A decays to 0 as the distance from the sources increases. The divergence between the seed predation scenarios (No predation, Proportional, Homogeneous with or without masting) is increased when x is not too large (i.e., around x_B). By contrast, with fat-tailed kernels, this difference is enhanced at large x, and the proportion π_A does not converge to 0 (Panels B and C in Fig. 4). More precisely, as x becomes very large, $J(x-x_A)/J(x-x_B)$ converges to 1 with the fat-tailed kernels J_{f_1} and J_{f_2}. Thus, very far from the two sources, π_A converges to $s(x_A)/(s(x_A)+s(x_B))$. In scenarios of no seed predation or proportional seed predation, this implies that π_A converges to $a(x_A)/(a(x_A)+a(x_B)) \approx 0.73$ with the parameter values of Fig. 4.

With the scenario of homogeneous seed predation, formula (14) implies that:

$$\lim_{x\to+\infty} \pi_A = \frac{a(x_A)}{a(x_A) + a(x_B)\frac{1+\theta\mu/a(x_A)}{1+\theta\mu/a(x_B)}},$$

which is approximately 0.81 with the parameter values of Fig. 4. Similarly, the limit of π_A can be computed explicitly from eq. (15) in scenario of homogeneous seed predation with masting,

leading to an intermediate value between those obtained in scenarios of no seed predation or scenario of homogeneous seed predation without masting: with the parameter values of Fig. 4, we get $\lim_{x\to+\infty} \pi_A \approx 0.77$. With the fat-tailed kernel J_{f_1} (Panel B in Fig. 4), the proportion π_A is minimal around x_B. This is due to the "peaked" nature of the kernel J_{f_1}: many seeds from the source x_B are dispersed very close to x_B. With the fat-tailed kernel J_{f_2} (Panel C in Fig. 4), this effect vanishes, as the seed dispersal is less concentrated around the sources.

3.3 Distribution of seed sources: effect of seed predation, masting and dispersal kernel

We now analyse for each seed predation scenario (no predation, homogeneous and proportional, same assumptions as in Section 3.2), and for each type of seed dispersal kernel, the distribution $m_x(y)$ (see eq. (9)) of the positions y of the sources of viable seeds arrived at each position x. This leads to the 2D graph presented in Fig. 5.

With a thin-tailed kernel (Panels A, B, C in Fig. 5), for all scenarios of seed predation with or without masting, depending on the position x, the main contributors are either seed sources from the core of the population (y in $(-10, 10)$) for lower values of x or from the front ($y > 10$) for higher values of x. In scenario of homogeneous seed predation, with or without masting, seed sources from the core remain the main contributors (i.e., a majority of viable seeds received at the position x come from parents y in $(-10, 10)$) until positions x which are about twice larger than in scenarios of no seed predation or proportional seed predation ($\approx$ 60m vs. 30m). At positions further away from the core, a lag appears between the position x and the position of the main contributors to the position x (see e.g. the dashed line vs. the mode of the distribution in Fig. 5). This gap is about twice larger in scenario of homogeneous seed predation without masting than in scenarios of no seed predation or proportional seed predation (45m vs. 22m), but this effect of seed predation is largely attenuated in the presence of masting (23m).

With a fat-tailed seed dispersal kernel of type 1 (Panels D, E, F in Fig. 5), the main contributors at a position x are either sources close to this position (the mode of the distribution remains close to the dotted line, i.e., $y \approx x$ for small x), or sources from the core of the population ($y \in (-10, 10)$ for larger x). In this case, the dispersal distance does not limit seed sources' contributions as viable seeds far away from the core ($x \gg 1$) may originate from contributors located in the core.

The main effect of scenario of homogeneous seed predation is a strong increase in the relative contribution of the individuals from the core at large x: about 60% of the contributors originate from the core in this scenario (without masting) vs. about 40% in scenarios of no seed predation or proportional seed predation. In the presence of masting, the contribution of the core of the population is about 50%. For large x, the same effect is observed with a fat-tailed kernel of type 2 (Panels G, H, I in Fig. 5), but the local effect of the contribution of seed sources located close to x is attenuated for smaller x due to the less peaked nature of the kernel.

4 Proofs

Proof of Lemma 1. We recall the Hardy-Littlewood rearrangement inequality (Theorem 368 in [22]). Consider two finite nonnegative sequences $x_1, \ldots, x_n$ and $y_1, \ldots, y_n$, arranged by increasing order, i.e., $0 \le x_1 \le x_2 \le \ldots \le x_n$ and $0 \le y_1 \le y_2 \le \ldots \le y_n$. Then, for any permutation $x_{\sigma(1)}, \ldots, x_{\sigma(n)}$, we have:

$$x_1\, y_n + x_2\, y_{n-1} + \ldots + x_n\, y_1 \le x_{\sigma(1)}\, y_1 + \ldots + x_{\sigma(n)}\, y_n \le x_1\, y_1 + \ldots + x_n\, y_n.$$

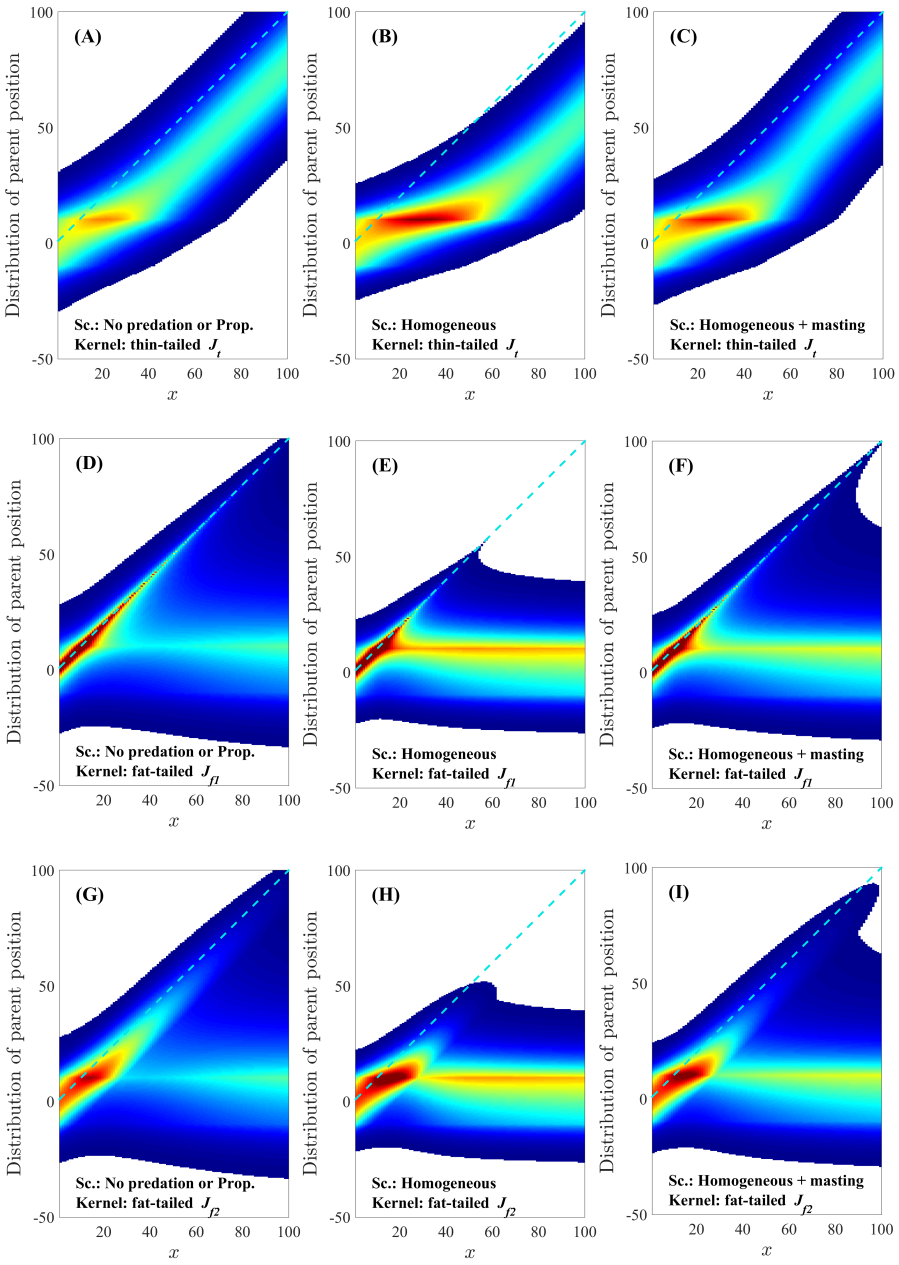

Fig. 5 Distribution $m_x(y)$ (see (9)) of the positions y of the sources of viable seeds arrived at x. The vertical axis is the location of the source y, and the horizontal is the location of the descendent seed x. The dashed line is the "first bisector" for which seed sources and viable seeds are located at the same position. Above this line, the seed sources positions are located in front of the seeds, while below the bisector the seed sources are located behind the seeds. Each seed predation scenario is depicted in each panel listed from A to I (in columns are presented the different scenarios and in rows are presented the three dispersal kernels i.e. thin-tailed kernel J_t and fat-tailed kernels J_{f_1} and J_{f_2}). For illustrative purposes, we do not show x positions below 0. The densities of viable seeds produced at a position y, $s(y)$ and $\overline{s}(y)$ are given by formulas (6) and (7). Colour bars represent the probability density of $m_x(y)$. In the presence of masting, the individual seed production r_k has the same sinusoidal shape as in Fig. 3.

In other words, the sum of the term-by-term products of the two sequences reaches its maximum when the sequences are arranged in the same order, and reaches its minimum when the sequences are arranged in opposite orders. Additionally, the inequalities are strict if the numbers are different ($x_1 < x_2 < \ldots < x_n$ and $y_1 < y_2 < \ldots < y_n$) and the permutation is not the identity nor the reversing-order permutation.

Consider the individual seed production $r_1, \ldots, r_n$ over one period (here, $n = T$). Without loss of generality, we can assume that the values are arranged in ascending order after a permutation of the indices has been applied. Set $x_1 = 1/r_n, \ldots, x_n = 1/r_1$, and $y_1 = r_1^2, \ldots, y_n = r_n^2$. Then, $x_1\, y_n + x_2\, y_{n-1} + \ldots + x_n\, y_1 = r_1 + \ldots + r_n = T\,\overline{r}$. The Hardy-Littlewood rearrangement inequality then shows that, for any permutation $x_{\sigma(1)}, \ldots, x_{\sigma(n)}$, we have:

$$T\,\overline{r} \leq \sum_{k=1}^{T} \frac{r_k^2}{r_{\sigma(k)}}.$$

In particular, with $\sigma(k) = k - d$, this shows that:

$$\overline{r} \leq \frac{1}{T} \sum_{k=1}^{T} \frac{r_k^2}{r_{k-d}}.$$

Proof of Lemma 2. Now, we prove a less classical inequality, which shows that in Scenario of homogeneous seed predation with masting, the mean number of healthy seeds per plant is always greater than (or equal) to that in the absence of masting. Consider again two finite nonnegative sequences $x_1, \ldots, x_n$ and $y_1, \ldots, y_n$, arranged by increasing order. We show that for any permutation $x_{\sigma(1)}, \ldots, x_{\sigma(n)}$, and $\alpha > 0$:

$$\sum_{k=1}^{n} \frac{y_k^2}{y_k + \alpha\, x_k} \leq \sum_{k=1}^{n} \frac{y_k^2}{y_k + \alpha\, x_{\sigma(k)}}. \tag{16}$$

In that respect, assume that the sequence $x_{\sigma(1)}, \ldots, x_{\sigma(n)}$ is not arranged in ascending order. Then, there are two indices i and j such that $y_i \leq y_j$ and $x_{\sigma(i)} > x_{\sigma(j)}$. Since

$$\begin{aligned}
&\frac{y_i^2}{y_i + \alpha x_{\sigma(i)}} + \frac{y_j^2}{y_j + \alpha x_{\sigma(j)}} - \left(\frac{y_i^2}{y_i + \alpha x_{\sigma(j)}} + \frac{y_j^2}{y_j + \alpha x_{\sigma(i)}} \right) \\
&\quad = \alpha^2 \frac{(y_j - y_i)(x_{\sigma(i)} - x_{\sigma(j)})(\alpha x_{\sigma(i)} x_{\sigma(j)} y_i + \alpha x_{\sigma(i)} x_{\sigma(j)} y_j + x_{\sigma(j)} y_i y_j + x_{\sigma(i)} y_i y_j)}{(\alpha x_{\sigma(i)} + y_i)(\alpha x_{\sigma(j)} + y_j)(\alpha x_{\sigma(j)} + y_i)(\alpha x_{\sigma(i)} + y_j)} \geq 0
\end{aligned}$$

we decrease the sum in the right hand side of (16) by exchanging $x_{\sigma(i)}$ and $x_{\sigma(j)}$. A finite number of similar exchanges leads a sequence $x_{\sigma(k)}$ arranged in ascending order, i.e., σ is the identity. This shows the rearrangement inequality (16).

Setting $\alpha = \theta\mu/a(x)$, $x_1 = r_1, \ldots, x_n = r_n, y_1 = r_1, \ldots, y_n = r_n$, and $n = T$, we obtain:

$$\sum_{k=1}^{T} \frac{r_k^2\, a(x)}{r_k\, a(x) + \theta\, \mu\, r_k} \leq \sum_{k=1}^{T} \frac{r_k^2\, a(x)}{r_k\, a(x) + \theta\, \mu\, r_{\sigma(k)}}.$$

which can be simplified into:

$$\frac{a(x)}{a(x) + \theta\, \mu} \sum_{k=1}^{T} r_k \leq \sum_{k=1}^{T} \frac{r_k^2\, a(x)}{r_k\, a(x) + \theta\, \mu\, r_{\sigma(k)}}.$$

Diving by T, and with $\sigma(k) = k - d$ we get:

$$\frac{\overline{s}(x)}{a(x)} = \frac{1}{T}\sum_{k=1}^{T} \frac{r_k^2\, a(x)}{r_k\, a(x) + \theta\, \mu\, r_{k-d}} \geq \overline{r} \frac{a(x)}{a(x) + \theta\, \mu}. \tag{17}$$

Proof of Lemma 3. We prove another non-standard result. Consider a finite nonnegative sequence $x_1, \ldots, x_n$ and a permutation $x_{\sigma(1)}, \ldots, x_{\sigma(n)}$. Then, consider the function:

$$H(\alpha) = (1 + \alpha) \sum_{k=1}^{n} \frac{x_k^2}{x_k + \alpha x_{\sigma(k)}}.$$

Differentiating $H(\alpha)$ with respect to $\alpha > 0$, we get:

$$H'(\alpha) = \sum_{k=1}^{n} \frac{x_k^2 (x_k - x_{\sigma(k)})}{(x_k + \alpha x_{\sigma(k)})^2}. \tag{18}$$

Our goal is to show that $H' \geq 0$. We assume without loss of generality that $x_1, \ldots, x_n$ is arranged in ascending order. Assume that the permutation $x_{\sigma(1)}, \ldots, x_{\sigma(n)}$ is not arranged in ascending order. Then, there are two indices i and j such that $\sigma(i) = j$, $x_i \leq x_j$ and $x_{\sigma(i)} > x_{\sigma(j)}$. Set $\sigma(j) = m$ and consider the difference between $H'(\alpha)$ before and after the pairwise permutation of $x_{\sigma(i)}$ and $x_{\sigma(j)}$:

$$\begin{aligned}
&\frac{x_i^2 (x_i - x_{\sigma(i)})}{(x_i + \alpha\, x_{\sigma(i)})^2} + \frac{x_j^2 (x_j - x_{\sigma(j)})}{(x_j + \alpha\, x_{\sigma(j)})^2} - \left(\frac{x_i^2 (x_i - x_{\sigma(j)})}{(x_i + \alpha\, x_{\sigma(j)})^2} + \frac{x_j^2 (x_j - x_{\sigma(i)})}{(x_j + \alpha\, x_{\sigma(i)})^2} \right) \\
&\qquad = \frac{x_i^2 (x_i - x_j)}{(x_i + \alpha x_j)^2} + \frac{x_j^2 (x_j - x_m)}{(x_j + \alpha x_m)^2} - \frac{x_i^2 (x_i - x_m)}{(x_i + \alpha x_m)^2} \\
&\qquad = \frac{\alpha (x_j - x_i)(x_j - x_m)}{(x_i + \alpha x_j)^2 (x_j + \alpha x_m)^2 (x_i + \alpha x_m)^2} F,
\end{aligned}$$

with F a polynomial with only positive terms:

$$\begin{aligned}
F = {} & \alpha^3 x_m^2 [x_i^2 (x_j + x_m) + x_j^2 (x_i + x_j)] + 2\alpha^2 x_i x_m (x_i^2 x_m + x_i x_j^2 + 2 x_i x_j x_m + x_j^3 + x_j^2 x_m) \\
& + \alpha x_i^2 (4 x_i x_j x_m + x_i x_m^2 + x_j^3 + 5 x_j^2 x_m + x_j x_m^2) + 2 x_i^3 x_j (x_j + x_m).
\end{aligned}$$

As $x_i \leq x_j$ and $x_j = x_{\sigma(i)} > x_{\sigma(j)} = x_m$, the above equation is positive (≥ 0). Thus, the pairwise permutation of $x_{\sigma(i)}$ and $x_{\sigma(j)}$ leads to a decrease of the sum in (18). With a finite number of such permutations, the sequence $x_{\sigma(1)}, \ldots, x_{\sigma(n)}$ can be rearranged into an increasing sequence, i.e., the sequence $x_1, \ldots, x_n$. We conclude that

$$H'(\alpha) = \sum_{k=1}^{n} \frac{x_k^2 (x_k - x_{\sigma(k)})}{(x_k + \alpha x_{\sigma(k)})^2} \geq \sum_{k=1}^{n} \frac{x_k^2 (x_k - x_k)}{(x_k + \alpha x_k)^2} = 0.$$

Setting $\alpha_A = \theta\mu / a(x_A)$, $\alpha_B = \theta\mu / a(x_B)$, $x_1 = r_1, \ldots, x_n = r_n, \sigma(k) = k - d$, and $n = T$, with $a(x_A) > a(x_B)$, we have $\alpha_A < \alpha_B$, and since H is increasing, $H(\alpha_A) \leq H(\alpha_B)$, which means that:

$$(1 + \theta\mu / a(x_A)) \sum_{k=1}^{n} \frac{r_k^2}{r_k + \theta\mu r_{k-d} / a(x_A)} \leq (1 + \theta\mu / a(x_B)) \sum_{k=1}^{n} \frac{r_k^2}{r_k + \theta\mu r_{k-d} / a(x_B)},$$

which in turns implies that:

$$\frac{\frac{1}{T}\sum_{k=1}^{T}\frac{r_k^2}{r_k+\theta\,\mu\,r_{k-d}/a(x_A)}}{\frac{1}{T}\sum_{k=1}^{T}\frac{r_k^2}{r_k+\theta\,\mu\,r_{k-d}/a(x_B)}} \leq \frac{1+\theta\,\mu/a(x_B)}{1+\theta\,\mu/a(x_A)}.$$

5 Discussion

Our study reveals the potential for predispersal seed predation, reproductive strategies (masting or non-masting) and seed dispersal patterns to jointly drive the diversity of seed sources in expanding plant populations. We provide theoretical support for possible evolutionary implications of predispersal seed predation in plant populations as its associated Allee effects in the colonisation front may lower the erosion of overall genetic diversity by reducing founder effects. In the presence of an Allee effect, the lower reproductive success of front individuals results in their lower contribution to the gene pool in the expansion front. It increases the relative contribution of core individuals, which consequently contribute to drive the dynamics of the expansion process. After several generations, this should enhance the maintenance of the genetic diversity towards the front as a result of pushed colonisation waves [39,53]. In the absence of an Allee effect, front individuals are expected to predominantly drive the dynamics of expansion process, leading to the 'surfing phenomenon' [14] associated with pulled colonisation waves [17,53] after several generations. This progressively leads to a loss of genetic diversity towards the expansion front due to successive founder effects [47,49,58]. It is worth noting that an Allee effect induced by predation could potentially co-occur with other factors that can create an Allee effect in the plant population, such as inbreeding depression [37].

Allee effects induced by predispersal seed predation depends on the foraging strategy. We show that different spatial patterns of seed predation have contrasted implications on the occurrence or the absence of seed predator-induced Allee effects in the expanding plant population. Here, Allee effects occur when there is a positive correlation between plant population density and plant individual reproductive success, i.e. when seed predation rates are higher at the front, where plant density is lower, than at the core of the plant population, where plant density is higher. This occurs in case of a uniform distribution of seed predator density across the expanding plant population (scenario of homogeneous seed predation), as well as in case of seed predator aggregation at the expansion front, i.e. in the low plant density area (scenario of sublinear seed predation). An Allee effect also occurs in case of seed predator aggregation within the core, i.e. in the high plant density area, but only when the positive correlation between predator and plant density is 'mild' (sublinear). In the latter case, the highest seed predator densities occur in the core, but the seed predation rate, i.e. the ratio between predator density and seed production, remains higher in the front, which generates an Allee effect. Conversely, no Allee effect occurs when considering a linear or a superlinear dependence in seed predator density with plant density. A linear dependence results in uniform seed predation rates across the plant population, making the individual plant reproductive success independent of the plant density. Superlinearity results in higher seed predation rates in the core, which negatively correlates individual reproductive success to plant density.

Therefore, our results show that the relationship between the densities of insect herbivores and their host plants determines the occurrence and magnitude of a biotic Allee effect. Various relationships between plant and insect distributions have been documented in different insect-plant systems, and our model covers all these situations. Insect attacks may indeed increase as the density of trees increases [44,51,52,56,59] or decreases [13,28,44,45,64]. Insect attacks may also

not depend on host density [13]. The Allee effect can be classified as weak or strong depending on the sign of the per capita growth rate at low plant densities [9]. Our model only considers the viable seed production rate and does not account for plant mortality, so additional assumptions are needed to determine the nature of the Allee effect. However, in the case of homogeneous seed predation, or more generally with Assumption 3, and assuming that $\mu(a)/a \to +\infty$ as $a \to 0$, the ratio s/a approaches zero as plant density a decreases. Assuming a constant mortality rate, this implies that the per capita growth rate will be negative, leading to a strong Allee effect.

Seed dispersal and masting modulate the seed predation-induced Allee effect. We showed that pivotal biological traits such as reproductive strategies (masting or non-masting) and seed dispersal (amount of long-distance dispersal) affect the strength of seed-predation-driven Allee effects . Based on rearrangement inequalities, we demonstrated that the mean number of viable seeds per plant was always larger in a masting population compared to a non-masting one in case of a seed predation scenario that leads to an Allee effect. This is true when the same total number of seeds is produced by both a masting species and a non-masting species over the same reproductive period. Thus, masting reduces the strength of the Allee effect due to overall lower predation rates at the front. From an evolutionary perspective over several generations, our model revealed that masting counterbalances the impact of seed predators on the founder effects and suggests an overall reduction of genetic diversity at the expansion front by limiting the contribution of core seed sources. This result brings new insights on the evolutionary potential of masting for plant populations, which has been the subject of an abundant literature [25,26,46].

Note that our model assumes a spatially constant seed production per plant r. However, less favourable conditions at the expanding edge might result in lower seed production, or conversely, if the plants at the forefront are fitter due to an evolutionary process, they might produce more seeds. In either case, this would result in a local seed production rate $r(x)\,a(x)$. Actually, this spatial variability would not affect our results since it can be artificially incorporated into the plant density $a(x)$, as long as it remains a decaying function away from $x = 0$.

Another interesting outcome of our theoretical approach is how seed dispersal patterns affect seed-predation-driven Allee effects. Examining diverse convolution kernels allowed us to analyse the relative contributions of core and front individuals along the expansion axis as well as the spatial origin of the main contributors for every position of dispersed seeds. With a thin-tailed kernel, the occurrence of an Allee effect sensibly increased the contribution of core seeds to the seed rain. This was shown by their higher mean propagation distances, which was found to be approximately twice larger with an Allee effect in our simulations. This is in line with an Allee-driven pushed wave of colonisation as previously mentioned. However, as thin-tailed kernels generally allow a relatively limited range of propagule dispersal, front contributors still prevail at the leading edge of the expansion. This contrasts with the use of a fat-tailed kernel, which showed an enhancement of the contribution of core seeds to the expansion front in the presence of an Allee effect, whatever its exact shape (fat-tailed kernels J_{f_1} and J_{f_2}). Thus, fat-tailed kernels may reinforce the maintenance of genetic diversity along an expansion. Noteworthy, as the fat-tailed kernel J_{f_2} has a less peaked nature than the fat-tailed kernel J_{f_1}, we observe a higher proportion of long-distance dispersal with J_{f_2} than with J_{f_1}. Long-distance dispersal is already acknowledged to increase core contributions to expansion fronts [2,7,15,24,41,42], which was described as pushed waves of neutral genetic diversity during colonisation [4,5]. Here we show that such pushed wave patterns are increased by the combination of Allee effects driven by biotic interactions and long-distance dispersal.

Our study sheds new light on evolutionary processes occurring during expansions [18,21,39, 53], implying that the ecological process of biotic interaction may influence expansion success or failure. The assessment of the evolutionary consequences of such process will likely benefit

from further broader assessments of spatio-temporal dynamics of populations interacting with their environments as the alteration of the incidence and strength of biotic interactions by global change has important effects on the distribution and abundance of species [12]. For instance, demographic and genetic implications of biotic interactions are still overlooked and largely neglected in forest dynamics models [3,36], mainly because demographic and genetic assessments in long-lived organisms like trees face substantial experimental constraints in both time and space.

As with any model, our approach makes a number of simplifications, and further work is required to evaluate the full implications of our result. Here, we considered a short period of time, i.e. sub-generation time, so that the new seeds do not contribute to the plant population during this period. Formal testing of the maintenance of genetic diversity over time requires multi-generational approaches accounting for competition effects between plants, which can involve partial differential equations [18,23,53], integro-differential equations [5] or their discrete time counterpart [39] (see Appendix 2 for an example of reaction-diffusion model that mimics some of the processes described here, but over several generations and with an explicit description of the movement of seed predators). In this work, the distribution of plants shapes the distribution of predators. Another possible assumption would be that predator density does not depend on the spatial distribution of a, but rather on the distribution of seeds previously dispersed from which the predator emerges. In this case, the predator density $p(x)$ would depend on $J \star a$, the convolution between the dispersal kernel J and the plant density a. This assumption, justified for predators that remain close to their birthplace, would induce a nonlocal dependence of the production of healthy seeds on a, preventing certain calculations such as those of the differentials (10) and (12). However, certain aspects would remain unchanged, such as the special case where μ is constant (homogeneous seed predation). Finally, our model does not include any spatial environmental variation. Demogenetic processes during expansion interact with local adaptation processes in a heterogeneous environment [20]. In that context, the contribution of seed sources from the core has a dual effect: on the one hand, it reduces the founder effects and therefore maintains the diversity in the front, on the other hand, it brings possibly locally maladapted genotypes to the front. Regarding dual effects of long-distance dispersal in trees in the context of climate change, [33] concluded that the positive effects of gene flow dominates the negative effects of maladaptation. We posit that the assessment of dual demogenetic processes resulting from biotic interactions in plant populations would deserve further attention.

References

1. Altwegg, R., Collingham, Y.C., Erni, B., Huntley, B.: Density-dependent dispersal and the speed of range expansions. Diversity and Distributions **19**(1), 60–68 (2013)
2. Bohrer, G., Nathan, R., Volis, S.: Effects of long-distance dispersal for metapopulation survival and genetic structure at ecological time and spatial scales. J. Ecol. **93**(5), 1029–1040 (2005)
3. Boivin, T., Doublet, V., Candau, J.N.: The ecology of predispersal insect herbivory on tree reproductive structures in natural forest ecosystems. Insect Science **26**(2), 182–198 (2019)
4. Bonnefon, O., Coville, J., Garnier, J., Hamel, F., Roques, L.: The spatio-temporal dynamics of neutral genetic diversity. Ecological Complexity **20**, 282–292 (2014)
5. Bonnefon, O., Coville, J., Garnier, J., Roques, L.: Inside dynamics of solutions of integro-differential equations. Discrete & Continuous Dynamical Systems-B **19**(10), 3057 (2014)
6. Bourbeau-Lemieux, A., Festa-Bianchet, M., Gaillard, J.M., Pelletier, F.: Predator-driven component allee effects in a wild ungulate. Ecology letters **14**(4), 358–363 (2011)
7. Cain, M., Milligan, B., Strand, A.: Long distance seed dispersal in plant populations. Am. J. Bot. **87**(9), 1217–1227 (2000)
8. Chen, I.C., Hill, J.K., Ohlemüller, R., Roy, D.B., Thomas, C.D.: Rapid range shifts of species associated with high levels of climate warming. Science **333**(6045), 1024–1026 (2011)
9. Courchamp, F., Berec, L., Gascoigne, J.: Allee effects in ecology and conservation. Oxford University Press (2008)

10. Crone, E.E., McIntire, E.J., Brodie, J.: What defines mast seeding? spatio-temporal patterns of cone production by whitebark pine. Journal of Ecology **99**(2), 438–444 (2011)
11. Davis, M.B., Shaw, R.G.: Range shifts and adaptive responses to quaternary climate change. Science **292**(5517), 673–679 (2001). URL http://www.ncbi.nlm.nih.gov/pubmed/11326089
12. Dormann, C.F., Bobrowski, M., Dehling, D.M., Harris, D.J., Hartig, F., Lischke, H., Moretti, M.D., Pagel, J., Pinkert, S., Schleuning, M., et al.: Biotic interactions in species distribution modelling: 10 questions to guide interpretation and avoid false conclusions. Global ecology and biogeography **27**(9), 1004–1016 (2018)
13. Doublet, V., Gidoin, C., Lefèvre, F., Boivin, T.: Spatial and temporal patterns of a pulsed resource dynamically drive the distribution of specialist herbivores. Scientific reports **9**(1), 1–12 (2019)
14. Edmonds, C.A., Lillie, A.S., Cavalli-Sforza, L.L.: Mutations arising in the wave front of an expanding population. Proc Natl Acad Sci USA **101**(4), 975–979 (2004)
15. Fayard, J., Klein, E.K., Lefèvre, F.: Long distance dispersal and the fate of a gene from the colonization front. J Evol Biol **22**(11), 2171–2182 (2009). URL http://blackwell-s̄synergy.com/doi/abs/10.1111/j.1420-s̄9101.2009.01832.x
16. Garnier, J.: Accelerating solutions in integro-differential equations. SIAM J Math Anal **43**, 1955–1974 (2011)
17. Garnier, J., Giletti, T., Hamel, F., Roques, L.: Inside dynamics of pulled and pushed fronts. J Math Pures Appl **98**, 428–449 (2012)
18. Garnier, J., Lewis, M.A.: Expansion under climate change: the genetic consequences. Bulletin of Mathematical Biology **78**(11), 2165–2185 (2016)
19. Gascoigne, J.C., Lipcius, R.N.: Allee effects driven by predation. Journal of Applied Ecology **41**(5), 801–810 (2004)
20. Gilbert, K.J., Sharp, N.P., Angert, A.L., Conte, G.L., Draghi, J.A., Guillaume, F., Hargreaves, A.L., Matthey-Doret, R., Whitlock, M.C.: Local adaptation interacts with expansion load during range expansion: maladaptation reduces expansion load. The American Naturalist **189**(4), 368–380 (2017)
21. Hallatschek, O., Nelson, D.R.: Gene surfing in expanding populations. Theor Popul Biol **73**, 158–170 (2008)
22. Hardy, G., Littlewood, J., Pólya, G.: Inequalities. Cambridge Mathematical Library. Cambridge University Press (1988)
23. Holmes, E.E., Lewis, M.A., Banks, J., Veit, R.: Partial differential equations in ecology: spatial interactions and population dynamics. Ecology **75**(1), 17–29 (1994)
24. Ibrahim, K.M., Nichols, R.A., Hewitt, G.M.: Spatial patterns of genetic variation generated by different forms of dispersal during range expansion. Heredity **77**(3), 282–291 (1996). URL http://www.nature.com/doifinder/10.1038/sj.hdy.6880320
25. Kelly, D.: The evolutionary ecology of mast seeding. Trends in ecology & evolution **9**(12), 465–470 (1994)
26. Kelly, D., Sork, V.L.: Mast seeding in perennial plants: why, how, where? Annual review of ecology and systematics pp. 427–447 (2002)
27. Klein, E.K., Lavigne, C., Gouyon, P.H.: Mixing of propagules from discrete sources at long distance: comparing a dispersal tail to an exponential. BMC Ecology **6**(3) (2006)
28. Knight, K.S., Brown, J.P., Long, R.P.: Factors affecting the survival of ash (Fraxinus spp.) trees infested by emerald ash borer (Agrilus planipennis). Biological Invasions **15**(2), 371–383 (2013)
29. Kolb, A., Ehrlen, J., Eriksson, O.: Ecological and evolutionary consequences of spatial and temporal variation in pre-dispersal seed predation. Perspectives in Plant Ecology, Evolution and Systematics **9**(2), 79–100 (2007)
30. Kot, M.: Discrete-time travelling waves: ecological examples. Journal of Mathematical Biology **30**(4), 413–436 (1992)
31. Kot, M., Lewis, M., van den Driessche, P.: Dispersal data and the spread of invading organisms. Ecology **77**, 2027–2042 (1996)
32. Kramer, A.M., Drake, J.M.: Experimental demonstration of population extinction due to a predator-driven Allee effect. Journal of Animal Ecology **79**(3), 633–639 (2010)
33. Kremer, A., Ronce, O., Robledo-Arnuncio, J.J., Guillaume, F., Bohrer, G., Nathan, R., Bridle, J.R., Gomulkiewicz, R., Klein, E.K., Ritland, K., et al.: Long-distance gene flow and adaptation of forest trees to rapid climate change. Ecology letters **15**(4), 378–392 (2012)
34. Lefèvre, F., Boivin, T., Bontemps, A., Courbet, F., Davi, H., Durand-Gillmann, M., Fady, B., Gauzere, J., Gidoin, C., Karam, M.J., et al.: Considering evolutionary processes in adaptive forestry. Annals of Forest Science **71**(7), 723–739 (2014)
35. Lesser, M.R., Jackson, S.T.: Contributions of long-distance dispersal to population growth in colonising Pinus ponderosa populations. Ecology Letters **16**(3), 380–389 (2013)
36. Lischke, H., Löffler, T.J.: Intra-specific density dependence is required to maintain species diversity in spatio-temporal forest simulations with reproduction. Ecological Modelling **198**(3-4), 341–361 (2006)
37. Luque, G.M., Vayssade, C., Facon, B., Guillemaud, T., Courchamp, F., Fauvergue, X.: The genetic Allee effect: a unified framework for the genetics and demography of small populations. Ecosphere **7**(7), e01413 (2016)
38. Lutscher, F.: Density-dependent dispersal in integrodifference equations. J Math Biol **56**(4), 499–524 (2008). URL http://www.ncbi.nlm.nih.gov/pubmed/17851661

39. Marculis, N.G., Lui, R., Lewis, M.A.: Neutral genetic patterns for expanding populations with nonoverlapping generations. Bulletin of Mathematical Biology **79**(4), 828–852 (2017)
40. Maron, J.L., Crone, E.: Herbivory: effects on plant abundance, distribution and population growth. Proceedings of the Royal Society B: Biological Sciences **273**(1601), 2575–2584 (2006)
41. Nathan, R.: Long-distance dispersal of plants. Science **313**(5788), 786–788 (2006)
42. Nathan, R., Klein, E., Robledo-Arnuncio, J.J., Revilla, E.: Dispersal kernels, vol. 15. Oxford University Press Oxford, UK (2012)
43. Nathan, R., Muller-Landau, H.: Spatial patterns of seed dispersal, their determinants and consequences for recruitment. Trends Ecol Evol **15**(7), 278–285 (2000)
44. Nerlekar, A.N.: Seasonally dependent relationship between insect herbivores and host plant density in Jatropha nana, a tropical perennial herb. Biology Open **7**(8), bio035071 (2018)
45. Otway, S.J., Hector, A., Lawton, J.H.: Resource dilution effects on specialist insect herbivores in a grassland biodiversity experiment. Journal of Animal Ecology pp. 234–240 (2005)
46. Pearse, I.S., Koenig, W.D., Kelly, D.: Mechanisms of mast seeding: resources, weather, cues, and selection. New Phytologist **212**(3), 546–562 (2016)
47. Peter, B.M., Slatkin, M.: Detecting range expansions from genetic data. Evolution **67**(11), 3274–3289 (2013)
48. Petit, R.J., Hu, F.S., Dick, C.W.: Forests of the past: a window to future changes. Science **320**(5882), 1450–1452 (2008)
49. Pierce, A.A., Gutierrez, R., Rice, A.M., Pfennig, K.S.: Genetic variation during range expansion: effects of habitat novelty and hybridization. Proceedings of the Royal Society B: Biological Sciences **284**(1852), 20170007 (2017)
50. Pluess, A.R.: Pursuing glacier retreat: genetic structure of a rapidly expanding larix decidua population. Mol Ecol **20**(3), 473–485 (2011). URL `http://doi.wiley.com/10.1111/j.1365-s294X.2010.04972.x`
51. Rhainds, M., English-Loeb, G.: Testing the resource concentration hypothesis with tarnished plant bug on strawberry: density of hosts and patch size influence the interaction between abundance of nymphs and incidence of damage. Ecological Entomology **28**(3), 348–358 (2003)
52. Root, R.B.: Organization of a plant-arthropod association in simple and diverse habitats: the fauna of collards (Brassica oleracea). Ecological Monographs **43**(1), 95–124 (1973)
53. Roques, L., Garnier, J., Hamel, F., Klein, E.K.: Allee effect promotes diversity in traveling waves of colonization. Proc Natl Acad Sci USA **109**(23), 8828–8833 (2012)
54. Roques, L., Hosono, Y., Bonnefon, O., Boivin, T.: The effect of competition on the neutral intraspecific diversity of invasive species. J Math Biol **71**(2), 465–489 (2014)
55. Salisbury, E.J., et al.: The reproductive capacity of plants. Studies in Quantitative Biology. G. Bell & Sons, London (1942)
56. Sholes, O.D.: Effects of associational resistance and host density on woodland insect herbivores. Journal of Animal Ecology pp. 16–23 (2008)
57. Silvertown, J.W.: The evolutionary ecology of mast seeding in trees. Biological journal of the Linnean Society **14**(2), 235–250 (1980)
58. Slatkin, M., Excoffier, L.: Serial founder effects during range expansion: a spatial analog of genetic drift. Genetics **191**(1), 171–181 (2012)
59. Stephens, A.E., Myers, J.H.: Resource concentration by insects and implications for plant populations. Journal of Ecology **100**(4), 923–931 (2012)
60. Thomas, P.: Trees: their natural history. Cambridge University Press (2014)
61. Turchin, P.: Quantitative Analysis of Movement: Measuring and Modeling Population Redistribution in Animals and Plants. Sinauer, Sunderland, MA (1998)
62. Wang, M.H., Kot, M., Neubert, M.G.: Integrodifference equations, Allee effects, and invasions. Journal of Mathematical Biology **44**(2), 150–168 (2002)
63. Xia, J., Sun, S., Liu, G.: Evidence of a component Allee effect driven by predispersal seed predation in a plant (Pedicularis rex, Orobanchaceae). Biology Letters **9**(5), 20130387 (2013)
64. Yamamura, K.: Relation between plant density and arthropod density in cabbage fields. Population Ecology **41**(2), 177–182 (1999)

Appendix 1: exponential dispersal kernel

As mentioned in the main text, the thin-tailed or fat-tailed nature of exponential dispersal kernels (exponential power kernel with $\beta = 1$) is not completely clear. On the one hand, these kernels share several properties of thin-tailed kernels, especially when included in continuous-time integro-differential models of Fisher-KPP type. Contrary to fat-tailed kernels, they do not lead to accelerating propagation but to travelling waves with a constant speed of expansion

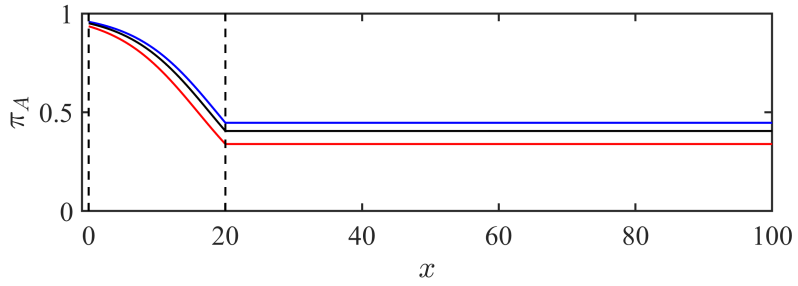

Fig. 6 Proportion π_A of seeds arriving in x from source x_A (at $x = 0$) compared to source x_B (at $x = 20$). Same legend as Fig. 4, but with the exponential dispersal kernel $J_e(x) = \frac{1}{2\,\alpha}\, e^{-\left(\frac{|x|}{\alpha}\right)}$, with $\alpha = 12$ (mean dispersal distance $\overline{d}(J_e) = \alpha = 12$m).

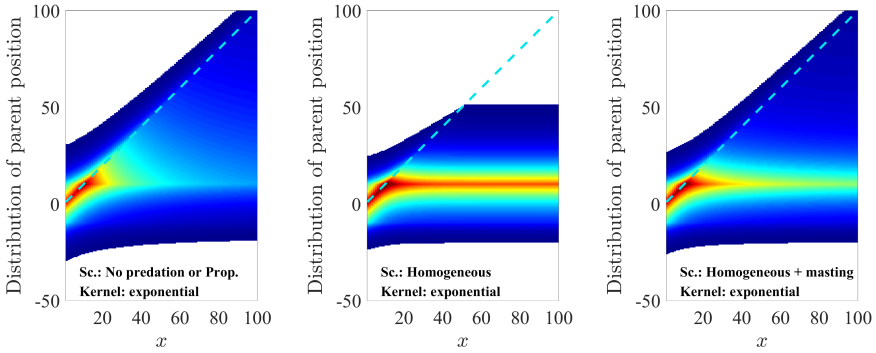

Fig. 7 Distribution $m_x(y)$ (see (9)) of the positions y of the sources of viable seeds arrived at x. Same legend as Fig. 5, but with the exponential dispersal kernel $J_e(x) = \frac{1}{2\,\alpha}\, e^{-\left(\frac{|x|}{\alpha}\right)}$, with $\alpha = 12$ (mean dispersal distance $\overline{d}(J_e) = \alpha = 12$m).

(see [16] and references therein). Additionally, still in the integro-differential framework, they lead to pulled propagation waves, meaning that they tend to limit the mixing of propagules to benefit individuals at the front of the wave [5]. On the other hand, with the exponential kernels $J_e(x) = \frac{1}{2\,\alpha}\, e^{-\left(\frac{|x|}{\alpha}\right)}$, we also observe that $J_e(x - x_A)/J_e(x - x_B) \to e^{(x_A - x_B)/\alpha} > 0$ as $x \to +\infty$. This means that, if we consider a discrete-time case or a single dispersal event, as observed in [27], and two sources at positions $x_A < x_B$, then these kernels lead to a mixing of propagules from both sources.

Within our framework of a single reproductive period (discrete-time), we expect exponential kernels to behave like fat-tailed kernels. To clarify what occurs in our specific context, we conducted the same computations as those leading to Figs. 4 and 5. The results clearly resemble the behaviour obtained with the fat-tailed kernel J_{f_1}, both for the proportion π_A of seeds arriving in x from source x_A (at $x = 0$) compared to source x_B (Fig. 6) and for the distribution $m_x(y)$ (9) of the positions y of the sources of viable seeds that arrived at x (Fig. 7).

Appendix 2: a toy reaction-diffusion model

In this appendix, we propose a reaction-diffusion framework that mimics some of the processes described in the main text, but over several generations and with an explicit description of the

movement of seed predators. In this framework, we assume continuous time and continuous space, with overlapping generations. Our objective is to test whether seed predation can lead to better maintenance of diversity over several generations, under basic assumptions about the movement of seed predators, and with other types of mathematical models than those in the main text.

In [53], we proposed a method to study the dynamics of neutral diversity during a colonisation process, with reaction-diffusion models. Our main result is that a standard Fisher-KPP growth term leads to an erosion of diversity, while the introduction of an Allee effect leads to a maintenance of diversity.

As in the main text, we denote by $a(t,x)$ the density of plants, here at time $t \in \mathbb{R}$ and position $x \in (-K, K)$ for some positive constant K ($K > L$). The density of seed predators is $p(t,x)$. We describe the plant - seed predator dynamics with the following system:

$$\begin{cases} \dfrac{\partial}{\partial t}a(t,x) = D_a \dfrac{\partial^2}{\partial x^2}a(t,x) + F(a,p), \\ \dfrac{\partial}{\partial t}p(t,x) = D_p \dfrac{\partial^2}{\partial x^2}p(t,x) + G(a,p), \end{cases} \quad t > 0,\ x \in (-K,K), \tag{A1}$$

with D_a, D_p the diffusion coefficients, which measures the mobility of the plants and seed predators, respectively, assuming a random walk movement which is described by the Laplace differential operator $\partial^2/\partial x^2$ (see e.g. [61]). Regarding the growth term F, we assume that:

$$F(a,p) = a(b(a,p) - d) - \gamma\, a^2, \text{ with } b(a,p) = b_0(1 - f(p/a)),$$

with $b \geq 0$ the plant birth rate, $d > 0$ the plant death rate, and f the proportion of predated seeds given by (5). In the absence of seed predators, $F(a,0)$ is a standard logistic (Fisher-KPP) growth term, with intrinsic growth rate $b_0 - d$ and a competition coefficient $\gamma > 0$. We then assume that the growth term associated with the seed predators has the form:

$$G(a,p) = \alpha\, a\, f(p/a) - \beta_1\, p - \beta_2\, p^2,$$

with $\alpha > 0$, so that the growth term is proportional to the local density of predated seeds $a\, f(p/a)$, and β_1, $\beta_2 > 0$ which correspond respectively to a death rate and a competition coefficient.

In order to track the dynamics of diversity in the plant population, we view it as the sum of a population whose ancestors come from the core a_c and of a population whose ancestors come from the forefront a_f, i.e., $a(t,x) = a_c(t,x) + a_f(t,x)$. At initial time, $a_c(0,x) = a(0,x)$ for $|x| \leq L$ and $a_c(0,x) = 0$ for $|x| > L$, and $a_f(0,x) = 0$ for $|x| \leq L$ and $a_f(0,x) = a(0,x)$ for $|x| > L$. We then use the method in [53] to describe the dynamics of a_c and a_f together with p:

$$\begin{cases} \dfrac{\partial}{\partial t}a_c(t,x) = D_a \dfrac{\partial^2}{\partial x^2}a_c(t,x) + \dfrac{a_c}{a}F(a,p), \\ \dfrac{\partial}{\partial t}a_f(t,x) = D_a \dfrac{\partial^2}{\partial x^2}a_f(t,x) + \dfrac{a_f}{a}F(a,p), \\ \dfrac{\partial}{\partial t}p(t,x) = D_p \dfrac{\partial^2}{\partial x^2}p(t,x) + G(a,p), \end{cases} \quad t > 0,\ x \in (-K,K). \tag{A2}$$

We note that, as expected, a ($= a_c + a_f$) and p satisfy the original system (A1). We assume Neumann (reflecting) boundary conditions at $\pm K$ ($\partial a_c/\partial x(t,\pm K) = \partial a_f/\partial x(t,\pm K) = \partial p/\partial x(t,\pm K) = 0$). The initial condition $a(0,x)$ is of the same form as in Fig. 1 (here, $a(x) = \exp(-2\,(|x| - L))$ for $|x| > L$ and $a(x) = 1$ in $(-L, L)$). The initial density of seed predators is $p(0,x) = 1$ for $|x| < L$ and $p(0,x) = 0$ for $|x| \geq L$ (or $p(0,x) \equiv 0$ in the absence of predation).

In Fig. 8, we depict the proportion of individuals from the core at time $t = 40$, $a_c/(a_c + a_f)$, depending on the presence of seed predators, and on the mobility of the seed predators. We

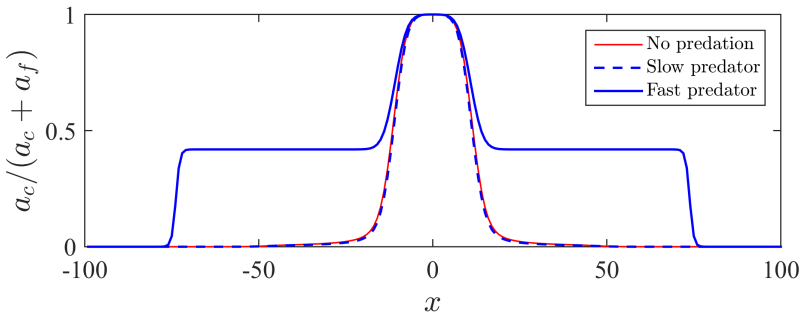

Fig. 8 Proportion of individuals from the core, with the reaction-diffusion model (A2)**, at time** $t = 40$**.** The parameter values are: $K = 100$, $L = 10$, $D_a = 0.1$, $D_p = 0.1$ (slow predator), $D_p = 1$ (fast predator), $b_0 = 2$, $d = 1$, $\alpha = 2$, $\beta_1 = \beta_2 = 1$, $\theta = 1/2$. The Matlab source code used to generate this figure is available at `https://doi.org/10.17605/OSF.IO/KWP4A`.

obtained this result by numerical simulation of the system (A2). In the absence of seed predators, or with slowly moving seed predators ($D_p = 0.1$), $a_c/(a_c + a_f)$ is close to 0 in the region $|x| > L$. On the contrary, when there is a fast seed predator ($D_p = 1$), the proportion $a_c/(a_c + a_f)$ reaches significant values even far from the core region $(-L, L)$. These preliminary results indicate that the presence of a fast enough predator reduces the initial advantage of the plants situated at the forefront and thereby leads to a better maintenance of plant diversity during the colonisation process. Interestingly, there appears to be a critical threshold for the rate of predator diffusion above which a_c is maintained during colonisation. Further work is needed to understand the role of masting (with e.g. delay-differential equations) and of long-distance dispersal (with e.g. integro-differential models) over several generations.